行政院國家科學委員會補助專題研究計畫成果報告

※※※※※※※※※※※※※※※※※※※※※※※※※
※　　　　　　　　　　　　　　　　　　　　　　　　※
※　具有序結構之金屬氧化物的合成與特性分析　※
※　　　　　　　　　　　　　　　　　　　　　　　　※
※※※※※※※※※※※※※※※※※※※※※※※※※

計畫類別：☑個別型計畫　　□整合型計畫

計畫編號：NSC 89-2113-M-002-059

執行期間：89 年 8 月 1 日 至 90 年 7 月 31 日

計畫主持人：劉如熹

本成果報告包括以下應繳交之附件：

□赴國外出差或研習心得報告一份

□赴大陸地區出差或研習心得報告一份

☑出席國際學術會議心得報告及發表之論文各一份

□國際合作研究計畫國外研究報告書一份

執行單位：台灣大學化學系

中 華 民 國 九十 年 五 月 二十三 日

行政院國家科學委員會專題研究計畫成果報告
具有序結構之金屬氧化物的合成與特性分析
Synthesis and characterization of metal-oxide compounds with ordered structures

計畫編號：NSC 89-2113-M-002-059
執行期限：89 年 8 月 1 日至 90 年 7 月 31 日
主持人：劉如熹 博士 （台灣大學化學系）
計畫參與人員：沈志鴻、詹丁山、王健源、張嵩駿、
黃明義、陳政琪、陳怡靜 （台灣大學化學系）

一、中文摘要

本研究第一部份，藉由同步輻射光探討 $LiMn_2O_4$ 材料之相變於 220 K 由立方體結構轉為長方晶系結構，利用鋰離子進出 MnO_6 中，形成離子導電化合物，而 $LiMn_{1.9}Co_{0.1}O_4$, 樣品由於 Co^{3+}之摻雜有效降低 Mn^{3+}含量進而抑制 Jahn-Teller 效應而於 25-300 K 則仍保持立方體結構。第二部份主要研究具有序雙層鈣鈦礦 (perovskite) 結構 $(Sr_{2-x}Ca_x)FeMoO_6$ (0 x 1.0) 樣品之晶體結構及磁性性質。由研究結果發現，晶格常數(*a* 與 *c*)值，隨鈣添加量的增加逐漸變小。磁化率隨 x = 0 至 x = 0.5 增加而於 x = 0.5 至 x = 1.0 少許降低，此複雜的磁性行為與化學壓力(相當於內壓)有很大之關聯。

關鍵詞：$LiMn_2O_4$、$LiMn_{1.9}Co_{0.1}O_4$、雙層鈣鈦礦、$(Sr_{2-x}Ca_x)FeMoO_6$.

一、Abstract

We have investigated the phase transition in spinel $LiMn_2O_4$ using powder synchrotron radiation diffraction and the crystal structure and magnetic properties of the new series of ordered double perovskite oxides $(Sr_{2-x}Ca_x)FeMoO_6$ (0 x 1.0). First, a transition from cubic (*Fd*3*m*) to orthorhombic (*Fddd*) was observed around T = 220 K in $LiMn_2O_4$. Increasing the average valence of Mn by doping Co ion into $[Mn_2O_4]$ framework, $LiMn_{1.9}Co_{0.1}O_4$, would reduce the concentration of the Mn^{3+}-ions, suppress the Jahn-Teller distortion and retain the cubic phase at low temperature 25-300 K. Second, a monotonous decrease of the lattice constants (*a* and *c*) has been found with increasing x in $(Sr_{2-x}Ca_x)FeMoO_6$. The magnetization increases from x = 0 to x = 0.5 and then slightly decreases from x = 0.5 to 1.0. Such complex magnetic behavior is strongly correlated to the chemical size effect (corresponding to the internal pressure) in the title compounds.

Keywords: $LiMn_2O_4$ 、 $LiMn_{1.9}Co_{0.1}O_4$ 、 Double perovskite、 $(Sr_{2-x}Ca_x)FeMoO_6$.

二、緣由與目的

Lithium transition-metal (Co, Ni, Mn, V) oxides which are used as positive electrodes in secondary lithium batteries have been extensively studied over the past two decades. Amongst these materials, manganese oxides were found to be advantageous promising in terms of specific energy, nontoxicity and low cost. Lithium spinel $LiMn_2O_4$ is the most promising candidate for innovative lithium-ion (rocking chair) batteries. It is believed that lithium manganese oxides batteries will be used in cellular telephones, notebook PCs and electrical vehicles in the future [1].

Some problems for the commercial application of $LiMn_2O_4$ are rechargeable capacity and poor cyclability of the charge-discharge process in the 4-V region. These could be due to the lattice instability of $LiMn_2O_4$ with the critical concentration of Mn^{3+} ions. $LiMn_2O_4$ shows cubic *Fd*3*m* symmetry at room temperature with an average manganese valence of 3.5. The Mn exists in Mn^{4+} ($t_{2g}^3e_g^0$) and Jahn-Teller active Mn^{3+} ($t_{2g}^3e_g^1$) configurations. Decreasing the temperature causes a structural phase transition around 280 K due to the Jahn-Teller distortion in the $Mn^{3+}O_6$ octahedra and the crystal structure of $LiMn_2O_4$ changes from cubic (*Fd*3*m*) to tetragonal (space group; *I*4$_1$/*amd*) [2,3]. Oikawa *et al.*[4] showed that the reflections of the low temperature phase in its neutron and X-ray diffraction patterns were indexed not on the basis of a tetragonal unit cell but roughly on an orthorhombic one (space group; *Fddd*) with lattice parameters *a* = 8.2797(2), *b* = 8.2444(3) and *c* = 8.1981(2) Å. Rodriguez-Carvajal *et al.*[5] on the basis of neutron and electron diffraction studies proposed an orthorhombic supercell with space group *Fddd* and ~3 x 3 x 1 axes with respect to the cubic value.

Yamada [3] has shown that the substitution of Li^+ ions at the Mn site, $Li(Li_xMn_{2-x})O_4$, increases the average ionic valence of Mn, thus decreasing the number of Jahn-Teller Mn^{3+} ions. When x > 0.035, the phase transition near room temperature was not observed. Towards practical applications, it is desirable to have a composition which has no structural transition close to room temperature.

The discovery of metallic ferromagnetism with large low-field room temperature magnetoresistance in

Sr_2FeMoO_6 by Kobayashi *et al.* [6] has stimulated research on double perovskite oxides. The magnetic structure of Sr_2FeMoO_6 was attributed to an ordered arrangement of parallel Fe^{3+} ($3d^5$, S = 5/2) magnetic moments, antiferromagnetically coupled with Mo^{5+} ($4d^1$, S = 1/2) spins. Since Fe^{3+} is in the high-spin state, its d orbitals are split into spin-up and spin-down states. The empty spin down states (π^*-β) of Fe^{3+} are degenerate to the one electron occupied spin down states (π^*-β) of Mo^{5+} which may lead to the formation of a narrow band. The electrons in this band have their spins antiparallel to the localized spins in the spin-up states (σ^*-α and π^*-α) of Fe^{3+}[7]. A ferromagnetic half-metallic state is observed in this ordered perovskite with localized up-spins of Fe^{3+} and itinerant down-spin electron of Mo^{5+}[8]. Many reports [8-11] are based on the results of the single substituent of A (A = Ba, Sr and Ca) in A_2FeMoO_6.

Here, we report the synthesis of $LiMn_{2-x}Co_xO_4$ (x = 0 and 0.1), wherein Mn has been partially replaced with Co ions and the effect of temperature on the phase transition in $LiMn_2O_4$ and $LiMn_{1.9}Co_{0.1}O_4$. We also present our studies on the variation of crystal structure and magnetic properties of the double perovskite system by chemical substitution of the smaller Ca^{2+} ions into the bigger Sr^{2+} sites (applying the internal anisotropic pressure) resulting in the system $(Sr_{2-x}Ca_x)FeMoO_6$ (0 x 1.0).

三、結果與討論

The low temperature structure of $LiMn_2O_4$ was investigated by powder synchrotron diffraction (λ= 1.3271 Å). The data were collected using an image plate from 300 K to low temperatures. Figure 1 shows the synchrotron powder diffraction profiles recorded from 300 K to 25 K. Peak-broadening is clearly seen in the pattern at 220 K, especially for the peaks at high-angles. The peaks at 11.17°, 18.35°, and 21.53° in 2θ are from grease (used to mount the sample on to the holder) and those at 33.13°, 39.28° and 45.07° are from the Be sample holder.

In *Fddd*, the corresponding Wyckoff positions are 8*a* (1/8, 1/8, 1/8), 16*d* (1/2, 1/2, 1/2) and 32*h* (x, y, z) [10]. The lattice constants are a = 8.242 Å for the cubic phase and a = 8.2797(2), b = 8.2444(3) and c = 8.1981(2) Å for orthorhombic phase [4], which have been calculated using the 2θ and (h k l) values obtained from the XRD patterns. In Fig. 2, we show the temperature dependence of the relative area of the (400) peak indexed by the space group *Fd*3*m* and the (004) peak indexed by *Fddd* phase for the $LiMn_2O_4$ sample. On cooling, the transformation to orthorhombic $LiMn_2O_4$ begins at 220 K and is complete at 210 K. The temperature of the structural transition shifts to 220 K which means that chemical substitution of Mn sites by the smaller Li^+ ($x \leq 0.026$) has taken place. The formula for our composition can be written as $Li(Li_{0.026}Mn_{1.974})O_4$. The Li ion substituting the Mn site increases the Mn valence and only by changing the Li and Mn ratio in the structure, the Mn valence changes in the $Li(Li_xMn_{2-x})O_4$ compositions. Yamaguchi *et al.*[2] have used X-ray absorption spectroscopy of the Mn K edge to investigate the valence state and local structure of $LiMn_2O_4$ at T = 280 K. The local structure is analyzed using isotropic $Mn^{4+}O_6$ and anisotropic $Mn^{3+}O_6$ octahedra in $LiMn^{3+}Mn^{4+}O_4$. The structure exhibits local ordering of the distorted $Mn^{3+}O_6$ octahedra when the temperature is below the transition temperature. The macroscopic distortion appears by ordering the local Jahn-Teller distortion below the transition temperature of 220 K [2]. Consequently, in the cubic phase above the transition temperature, the $Mn^{3+}O_6$ octahedra are distorted by the Jahn-Teller effect, which is a local distortion without static or dynamic order. Therefore, the charge ordering process is accompanied by the presence of an orbital ordering which is the manifestation of the Jahn-Teller polaronic nature of the mobile charge above and below the transition temperature [5]. By the method of chemical titration, we have determined the Mn valence of the $LiMn_2O_4$ sample to be 3.505 ± 0.004. The present results for increased Mn valences in our compound strongly suggest that a small amount of Li ions substitute for Mn at the octahedral site and that the value of x is less than 0.026.

The chemical substitution of Co^{3+} for Mn^{3+} in $LiMn_2O_4$ increases the Mn valence. The Mn valence of $LiMn_{1.9}Co_{0.1}O_4$, as determined by chemical titration, is 3.526 ± 0.006. Therefore, the $LiMn_{1.9}Co_{0.1}O_4$ composition can be written as $Li(Co^{3+}_{0.1}Mn^{3+}_{0.9}$-$Mn^{4+}_{1.0})O_4$. Yamada [3] has observed that the DSC peaks corresponding to the phase transition smeared out in $Li(Li^+_{0.035}Mn^{3+}_{0.895}Mn^{4+}_{1.07})O_4$. Figure 3 shows the synchrotron diffraction patterns of $LiMn_{1.9}Co_{0.1}O_4$ sample showing the cubic spinel peaks (333), (511), (440), and (531) in the 2θ range of 46 - 59° from 300 K down to 25 K. As can be seen, there is no peak split or broadening from room temperature to low temperature. The substitution effect of Co^{3+} on the framework would be local in 16*d* site, which is similar to excess Li^+ being substituted into the Mn site. In $LiMn_{1.9}Co_{0.1}O_4$, the Mn^{3+} content decreases to 47%, thus bringing about a change in the magnetic-ordering. As we can see, the Mn^{3+} Jahn-Teller distortion is small in $LiMn_{1.9}Co_{0.1}O_4$ at room temperature. However, at low temperature, the ordering of the distorted $Mn^{3+}O_6$ octahedra is quite small in $LiMn_{1.9}Co_{0.1}O_4$ as compared to the composition with $LiMn_2O_4$.

From the XRD measurements, it can be found that the samples of the series $(Sr_{2-x}Ca_x)FeMoO_6$ (0 x 1.0) are of single phase and can be indexed on the basis of a tetragonal unit cell with a space group of *I*4/*mmm*. The initial structural model to be refined with the Rietveld profile analysis is based on the model of Sr_2FeMoO_6 [8] (as shown in the inset of Fig. 4) by assuming that the Ca^{2+} ions substituted into the Sr^{2+} sites. Figure 4 displays the observed X-ray powder diffraction data at 300 K, along with the calculated diffraction patterns, of $(Sr_{2-x}Ca_x)FeMoO_6$ with x = 0.5. All the observed peaks satisfied the reflection conditions of the space group *I*4/*mmm*, $h + k + l$ =

even; *hk*0, *h* + *k* = even; and 00*l*, *l* = even. Refinement with this model yields a satisfactory fit to the overall profile with the reliability factors of R_p = 7.97%, R_{wp} = 11.89% and χ^2 = 1.47. The structural parameters and refined results from X-ray powder diffraction data at 300 K for the composition with x = 0.5 are tabulated in Table 1. The occupancies for the (Sr, Ca, O) sites were kept constant in our data refinements. Refinement of occupancy at Fe and Mo sites indicates that the odering of Fe and Mo atoms is 84 and 75%, respectively. Moreover, the Fe-O-Mo angle within a-b planes is reduced from 180º for x = 0 to 162º for x =1.0 which indicates a distorted structure in the Ca-rich sample. The lattice parameters (*a* and *c*) and cell volume (inset of Fig.5) decrease with increasing Ca content as shown in Fig. 5, which is due to the chemical substitution of the smaller Ca^{2+} ions (1.34 Å) into the bigger Sr^{2+} ionic (1.44 Å) sites [12].

In Fig. 6, we show the field dependence of magnetization at 5 K of $(Sr_{2-x}Ca_x)FeMoO_6$ (x = 0 , 0.5 and 1.0). The magnetization at 5 T per a formula unit of Sr_2FeMoO_6 is ~ 3.2 μ_B at 5 K, which is the same as that of the report by Tomioka et al. [8]. This satuation magnetization is less than the predicted value of 4.0 μ_B/formula unit. Goodenough et al [13] have suggested the existence of the antiphase boundary with antiferromagnetic coupling across the boundary due to the disordering of Fe and Mo, which may cause the decrease in magnetization as compared to the predicted value. XRD refinement indicates ~ 10 % disordering between Fe and Mo in our samples. The smaller size of Ca^{2+} distorts the structure of $(Sr_{2-x}Ca_x)FeMoO_6$. Our results show that in the tetragonal structure from x = 0 to x = 1.0, the Fe-O-Mo angle within the a-b planes decreases from 180 to 162º linearly. We propose that the complex variation of magnetization with Ca-doping in $(Sr_{2-x}Ca_x)FeMoO_6$ (0 ≤ x ≤ 1.0) may be strongly correlated to the reduction of bond angle of Fe-O-Mo. A detailed study of this aspect is still underway.

四、結論

In conclusion, we have carried out conventional and synchrotron powder X-ray diffraction studies of $LiMn_{2-x}Co_xO_4$ with x = 0 and 0.1. $LiMn_2O_4$ shows a phase transition at 220 K that is associated with cubic-orthorhombic distortion. Reduction of the concentration of the Mn^{3+}-ions results in the suppression of the Jahn-Teller distortion in $LiMn_{1.9}Co_{0.1}O_4$ and retains the cubic phase at low temperature. And we have studied the chemical size effect on the structure and magnetic properties of $(Sr_{2-x}Ca_x)FeMoO_6$ (0 ≤ x ≤ 1.0). Across the system, the materials are of single phase with the lattice parameters (*a* and *c*) and cell volume decreasing with increasing Ca content. Moreover, the magnetization increases from x = 0 to x = 0.5 and then slightly decreases from x = 0.5 to 1.0 which may be controlled by the chemical pressure via Ca-doping in Sr_2FeMoO_6.

五、計畫成果自評

We have reached the goals of the research plan, some part of the results have already publicized or in scientific journals [14-17].

六、參考文獻

[1] M. M. Thackeray et al., *Mater. Res. Bull,* 1983, **18**, 461.
[2] H. Yamaguchi et al, *Phys. Rev. B,* 1998, **58**, 8.
[3] A. Yamada et al., *J. Solid State Chem*, 1996, **122,** 160.
[4] K. Oikawa et al., *Solid State Ionics,* 1998, **109**, 35.
[5] J. Rodriguez-Carvajal et al., *Phys. Rev. Lett,* 1998, **81,** 4660.
[6] K. -I. Kobayashi et al., *Nature* , 1998, **395**, 677.
[7] A. W. Sleight et al., *J. Phys. Chem. Solids*, 1972, **33**, 679.
[8]Y. Tomioka et al., *Phys. Rev. B*, 2000, **61,** 422.
[9] A. Maignan et al., *J. Solid State Chem,* 1999, **14** 224.
[10] J. A. Alonoso et al., *Chem. Mater*, 2000, **12,** 161.
[11] T. Yamamoto et al., *J. Mater. Chem,* 2000, **10** 2342.
[12] R. D. Shannon et al., *Acta Crystallogr,* A, 1976, **32**, 751.
[13] J. B. Goodenough et al., *Inter. J. Inorg. Mater*, 2000, **2** , 3.
[14] C. H. Shen et al., *J. Chem. Soc., Dalton Trans.*, 2001, **1**, 37.
[15] R. S. Liu et al., *Solid State Commu.*, 2001, **118**, 367.
[16] C. H. Shen et al., *J. Power Sources*, 2001, in press.
[17] R. S. Liu et al., *Soild State Ionics,* 2001, in press.

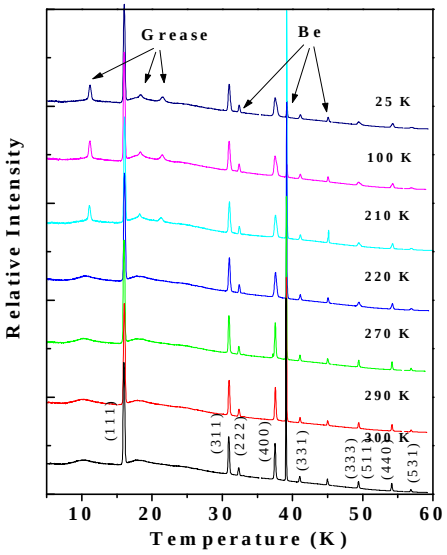

Fig. 1. Powder X-ray diffraction patterns of $LiMn_2O_4$, taken between 300 and 25 K

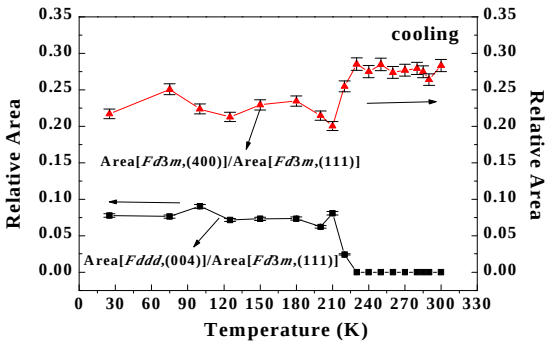

Fig. 2. Relative area as a function of the temperature in $LiMn_2O_4$.

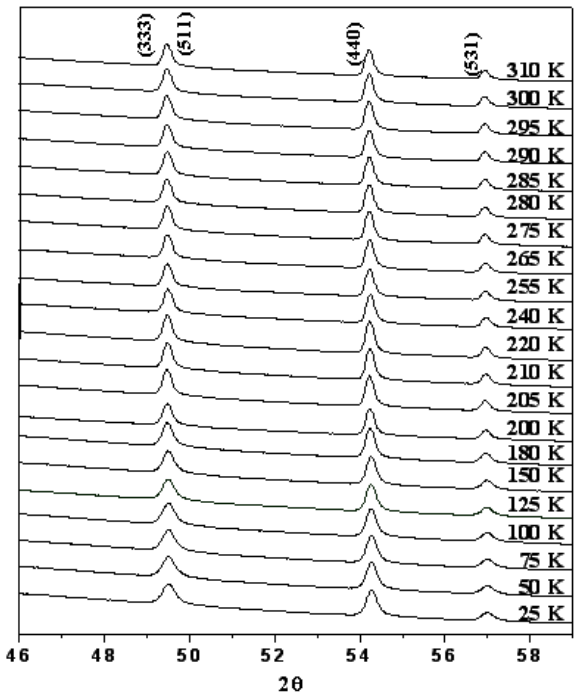

Fig. 3. Powder X-ray diffraction patterns of $LiMn_{1.9}Co_{0.1}O_4$ at 2θ of 46° ~ 59 ° region, taken between 300 and 25 K with synchrotron of wavelength 1.3271 Å.

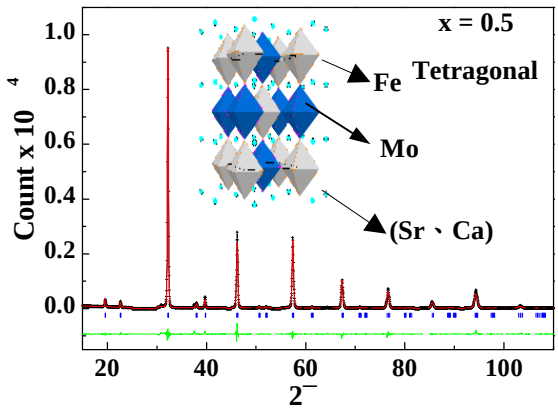

Fig. 4. Observed, calculated, and difference X-ray powder diffraction patterns of $(Sr_{2-x}Ca_x)FeMoO_6$ (x = 0.5) at 300 K. Reflection positions are marked for the ideal phase.

Table Ⅰ. Structural parameters and refined results from XRD data at 300 K of $(Sr_{2-x}Ca_x)FeMoO_6$ (x = 0.5).

$(Sr_{2-x}Ca_x)FeMoO_6$ (x = 0.5)					
Atom	*x*	*y*	*z*	10^2Uiso/(Å^2)	Fraction
Sr1	0.5	0	0.25	2.99(5)	0.778
Ca2	0.5	0	0.25	2.99(5)	0.222
Fe(3)	0	0	0	3.03(7)	0.838(9)
Mo(4)	0	0	0	3.03(7)	0.172(9)
Mo(5)	0.5	0.5	0	2.13(5)	0.749(1)
Fe(6)	0.5	0.5	0	2.13(5)	0.241(1)
O(7)	0.2472	0.2472	0.2025	2.40(1)	1
O(8)	0	0	0.2528(3)	3.01	1
Space group : *I*4 / *mmm* (tetragonal)					Reliability factors
Cell parameters:					R_p = 7.97 %
a = 5.5564(4) Å b = 5.5564(4) Å					R_{wp} = 11.89 %
c = 7.8824(5) Å					
Cell volume: 243.35(3) Å^3					χ^2 = 1.47

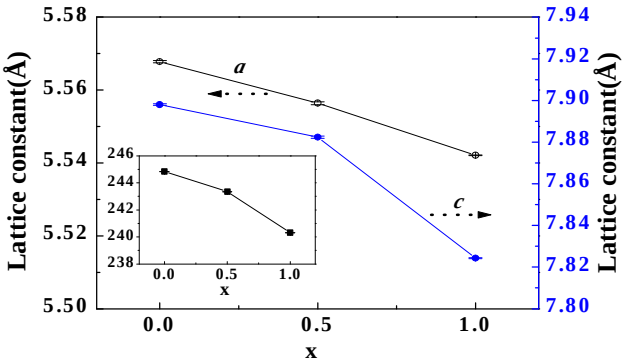

Fig. 5. Lattice constants (*a* and *c*) as a function of x in $(Sr_{2-x}Ca_x)FeMoO_6$ (x = 0 ~1.0). The cell volume as a function of x is shown in the inset.

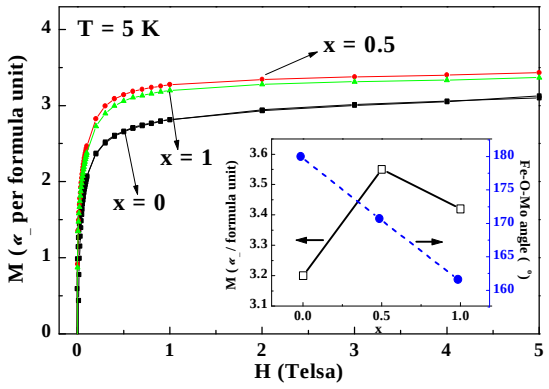

Fig. 6. Field dependence of magnetization at 5 K of $(Sr_{2-x}Ca_x)FeMoO_6$ (x = 0 , 0.5 and 1.0). The composition parameter x dependence of magnetization and Fe-O-Mo angle within a-b planesis shown in the inset.